Available online at www.sciencedirect.com
SCIENCE DIRECT®
PERGAMON
Vacuum 71 (2003) 193–199
VACUUM
SURFACE ENGINEERING, SURFACE INSTRUMENTATION & VACUUM TECHNOLOGY
www.elsevier.com/locate/vacuum

# Tunnelling spectroscopy of Pt nanoparticles supported on $TiO_2(1\,1\,0)$ surface

J. Szökő, A. Berkó*

*Reaction Kinetics Research Group, Hungarian Academy of Sciences, University of Szeged, P.O. Box 168, H-6701 Szeged, Hungary*

Received 16 June 2002; received in revised form 23 September 2002; accepted 30 September 2002

**Abstract**

Pt nanoparticles fabricated by metal vapour deposition were studied on $TiO_2(1\,1\,0)$ support as a function of their sizes by scanning tunnelling microscopy and spectroscopy (STM, STS). Two different procedures were applied for the fabrication of Pt nanoparticles: (i) deposition of the metal at room temperature followed by step by step annealing at higher temperatures; (ii) the growing of Pt seeds by deposition of Pt at 1100 K ("seeding + growing" method (J. Catal 182 (1999) 511). The *I–V* spectra recorded above the middle point of the Pt particles indicated that an increase in the average diameter of the nanoparticles does not result in a more metallic character. Moreover, the characteristic lineshape of the tunnelling spectra refers to an insulator character even for larger particles (> 5 nm). This behaviour was attributed to the formation of a decoration $TiO_x$ layer on the top facets of the Pt particles. It was also found that periodic current oscillation appears in the *I–V* curves recorded above Pt nanoparticles decorated partially. This phenomenon may be explained by the formation of electron traps at the metal/oxide interface capturing and emitting electrons from/to the tunnelling current.


*Keywords:* Pt; $TiO_2(1\,1\,0)$; STM-STS; Decoration; SMSI

## 1. Introduction

Scanning tunnelling microscopy (STM) and spectroscopy (STS) deliver information on the local electronic structure of the surfaces and are increasingly applied for atomic scale characterization of two-dimensional model catalysts [1,2]. Unfortunately, there are some limiting factors of the employment of the tunnelling spectroscopy in this field: (i) it can be used only in the energy range close to the Fermi level; (ii) the fine details of the *I–V* curves depend strongly on the local electronic state of the tip itself; (iii) the tunnelling spectra recorded above the supported nanoparticles exhibit chemical states of both the particle and the particle–support interface [1–3].

$I-V$ spectra taken on clean $TiO_2(1\,1\,0)$–$(1\times1)$, $(1\times2)$ and disordered surfaces at 300 K have shown that the zero-current range around the zero-bias became more restricted as the surface was more reduced [4]. This observation is in harmony with the assumption that the zero-current regime measures the width of the surface band gap. In the case of the supported clusters,

*Corresponding author. Tel.: +36-62544803; fax: +36-62424997.
*E-mail address:* aberko@chem.u-szeged.hu (A. Berkó).

0042-207X/03/$ - see front matter 
doi:10.1016/S0042-207X(02)00736-4

there are two barriers in series connection: between (i) the tip and the particle; (ii) the particle and the support. Assuming that the ad-particle is a clean metal cluster, the features on the *I–V* curves refer to the electron states of the particle/support interface. In the case of reducible oxides (as $TiO_2$), however, the high-temperature treatments in UHV induce the formation of a decoration (encapsulation) layer on the supported noble metal nanoparticles [11–15]. This behaviour may cause further complications in the understanding of the tunnelling current spectra.

In this work, Pt nanoparticles grown on $TiO_2$(1 1 0) surface (one of the best known SMSI system) were investigated as a function of the particle size by STM–STS.

## 2. Experimental

The experiments were performed in a UHV system equipped with an STM head, a quadrupole mass spectrometer and a CMA electron energy analyzer. A commercial $Ar^+$ gun was applied for cleaning the samples. The polished $TiO_2$(1 1 0) probe was clipped by Ta plates and mounted on a transferable sample cartridge. An Ohmically heated W filament served for annealing the probe. The temperature was checked by a chromel–alumel thermocouple sticked to the side of the sample by ceramobond. The cleaning procedure of the $TiO_2$(1 1 0) surface consisted of a few hours annealing at 900 K in UHV, some cycles of $Ar^+$ ion bombardment (10 m, 1.5 kV, $10^{-6}$ A cm$^{-2}$) at room temperature and annealing at 1200 K for 10 m. The purity of the surface was checked by Auger electron spectroscopy.

The STM imaging was performed by an electrochemically edged W tip. Bias of +1.5 V and current of 0.2 nA were typically used for imaging. Characteristic pictures and *I–V* spectra shown in this work were chosen from numerous records obtained on different regions of the sample. For detection of the *I–V* curves, the following parameters were applied: bias range of [−3, +3 V] tip-surface distance stabilized at 0.02 nA and +1.5 V, the recorded spectra were the sum of 8 scans above the same site.

## 3. Results and discussion

### 3.1. Fabrication of PT nanoparticles on a $TiO_2$(1 1 0)-(1 × n) support

The preparation of clean $TiO_2$(1 1 0)-(1 × n) surface was described in detail earlier [4,5]. The surface of the support is depicted by STM images of 100 nm × 100 nm in Fig. 1A. The 1D rows running in the orientation of [0 0 1] are separated by multiples ($n$) of 0.65 nm, where $n = 2, 3, 4$ they were attributed to a $Ti_2O_3$ phase formed on the top of (1 × 1) ordered $TiO_2$(1 1 0) surface [6–10]. For the fabrication of supported nanocrystallites, two different procedures were applied in this work: (i) deposition of the metal at 300 K followed by annealing at higher temperatures for 10 m; (ii) formation of Pt seeds by deposition of 1–2% ML (monolayer) of the metal at 300 K followed by annealing at 1100 K for 10 m and post-growing of the metal seeds by evaporation of additional metal at high temperature (1100 K). Figs. 1B–D depict the characteristic morphology of the $TiO_2$(1 1 0) surface exposed to 1.5 ML of Pt at room temperature and annealed at different temperatures (B) 500 K; (C) 1000 K; (D) 1200 K. As it can be seen, Pt particles increase gradually: for the images B, C and D, the average diameter is 3, 5 and 7 nm, respectively. The ratio of height/diameter is approximately 0.25 for each case. The other series of the STM pictures refers to the "seeding + growing" procedure (Figs. 1E–H). In this case, the surface was exposed to 0.01 ML of Pt at 300 K with a subsequent annealing at 1100 K for 10 m ("seeding") (Fig. 1E). This step was followed by "growing" of the existing nanoparticles by deposition of additional metal at 1100 K (Figs. 1F–H) [16–18]. As can be seen, the average size of the Pt particles changed radically from 4–5 (E) upto 25–30 nm (H). The hexagonal outline and the flat top facet of the Pt particles suggest clearly that they possess a regular inner structure and an (1 1 1) oriented top facet. A recent paper by Dulub et al. revealed that the hexagonal coin-shaped Pt particles grown by deposition at 300 K followed by annealing at 1000 K for 30 m are covered by an ordered $TiO_{1.1}$ overlayer [14,15]. We have also demonstrated recently that the post-grown Pt

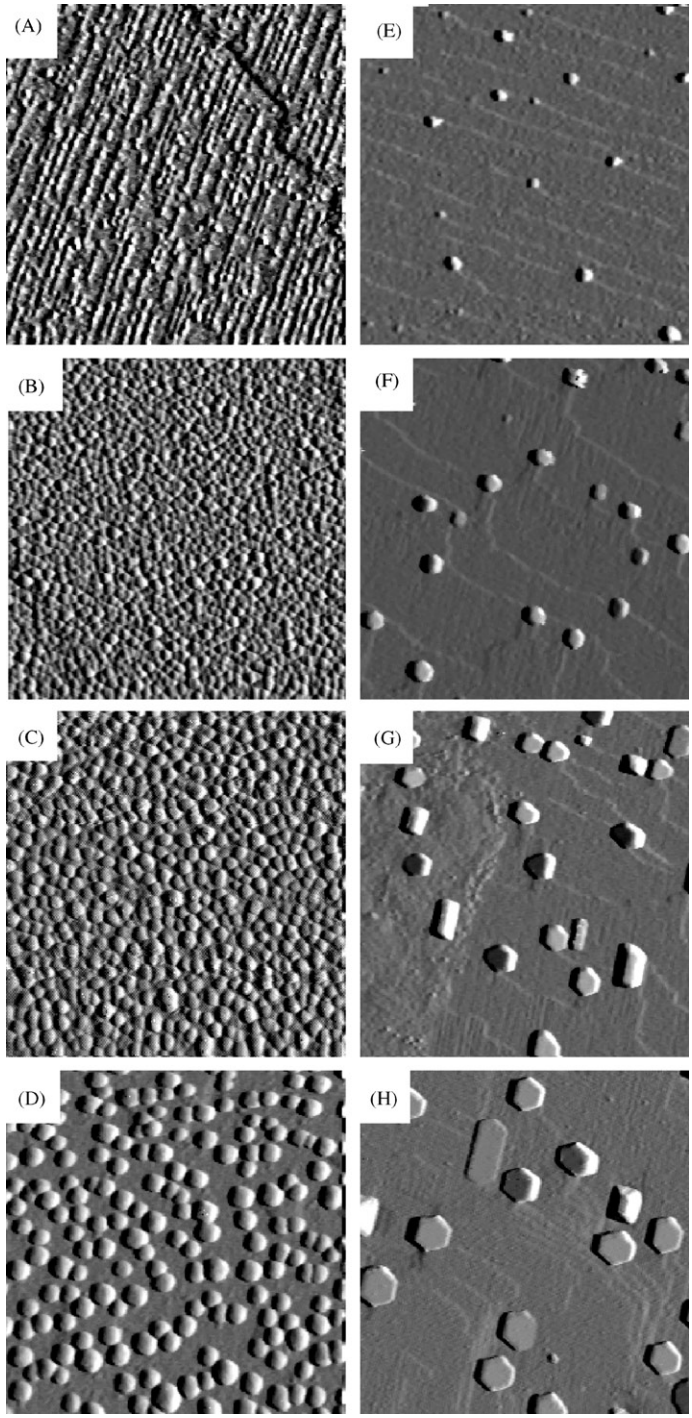


Fig. 1. STM images on the differently prepared $Pt/TiO_2(1\,1\,0)-(1\times n)$ surfaces. (A) The clean support before the deposition of Pt. The characteristic morphology after deposition of 1.5 ML of Pt at 300 K followed by annealing at (B) 500 K; (C) 1000 K; (D) 1200 K. Pt nanocrystallites of increasing sizes formed by the seeding and growing method. (E) Pt seeds formed by deposition of 0.01 ML Pt at 300 K followed by annealing at 1100 K post-growing of the Pt seeds by deposition of additional metal. (F) 0.25 ML, (G) 1.25 ML and (H) 2.8 ML at 1100 K. The size of the images (A–D) $100\times100$ nm, (E–H) 200 nm $\times$ 200 nm.

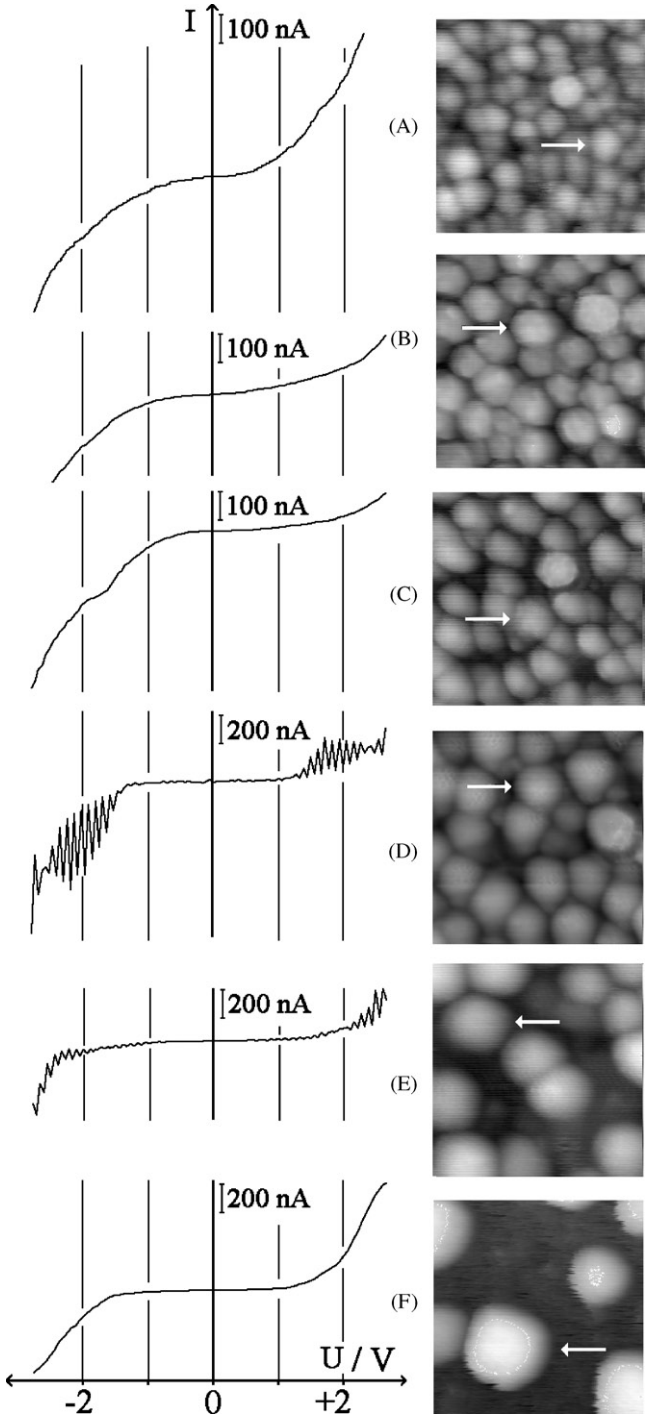


Fig. 2. Characteristic tunnelling spectra recorded above individual Pt crystallites (indicated by arrows) formed by deposition of 1.5 ML Pt at 300 K (A) and step by step annealing at higher temperatures (B) 700 K; (C) 900 K; (D) 1000 K; (E) 1100 K and (F) 1200 K. The average diameter of the particles for the different stages were: (A) 2.5 nm; (B) 2.9 nm; (C) 3.1 nm; (D) 3.8 nm; (E) 4.4 nm and (F) 6.3 nm. The size of the STM images is 20 nm × 20 nm.

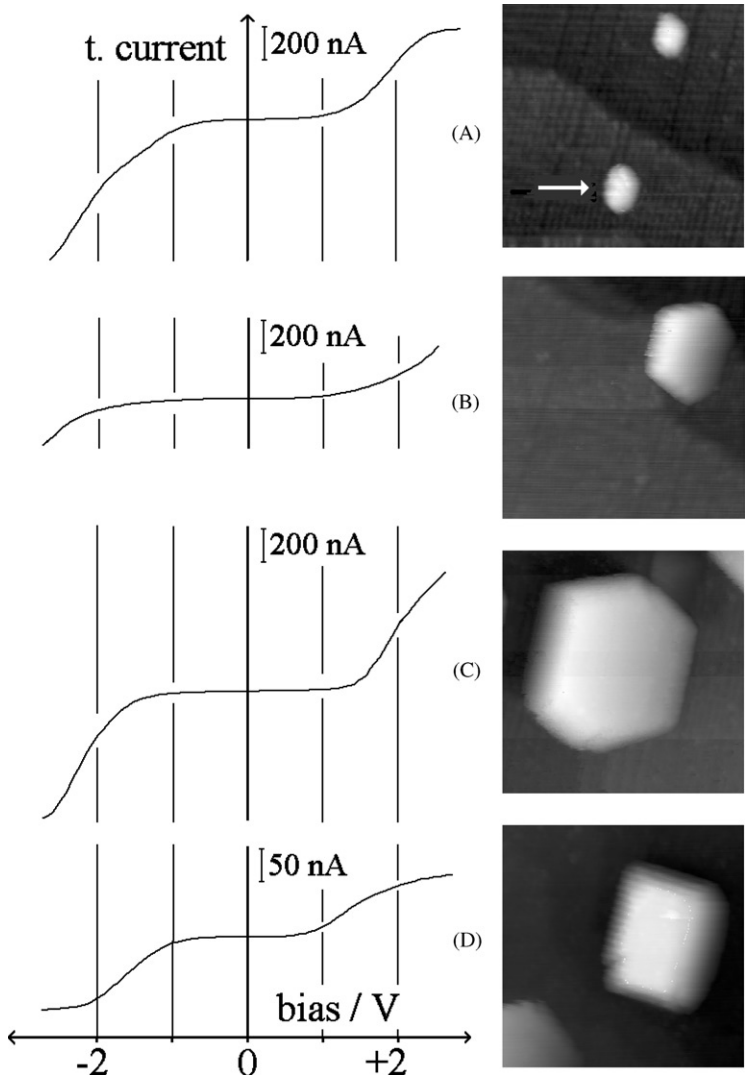


Fig. 3. Characteristic tunnelling spectra recorded above post-grown Pt crystallites of increasing diameter: (A) above a Pt seed of 6.1 nm (indicated by arrow) obtained by deposition of 0.01 ML Pt at 300 K followed by annealing at 1100 K for 10 m above post-grown hexagonal Pt crystallites of (B) 9.5 nm, (C) 28 nm and above a rectangular Pt crystallite of 17.5 nm. The size of the images is 50 nm × 50 nm.

nanoparticles (as in Figs. 1E–H) possess a decoration thin film [19].

### 3.2. *Tunnelling spectroscopy of the supported Pt nanoparticles of different sizes*

The *I–V* curves shown in Fig. 2 were detected above the Pt particles (indicated on the STM images) fabricated by the deposition of 1.5 ML Pt at room temperature and by annealing at different temperatures for 10 m. The particles of 2.5 nm size formed by deposition at 300 K exhibit a rather metallic character exhibiting a nearly zero band gap region (Fig. 2A). This behaviour changes only slightly on the effect of annealing at (B) 700 K and (C) 900 K and the average particle size increases by 50% (up to 3 nm). The annealing at 1000 K leads to the appearance of spectral features both in the

positive and the negative bias range (Fig. 2D). This periodic oscillation of the tunnelling current is centered at around –1.9 and +1.8 V. It is important to note that this is the same temperature range where the decoration of the Pt clusters proceeds [5]. In this way, the current oscillation may be connected to the formation of $TiO_x$ nanoclusters on the top facet of the Pt particles. An average size of 3.8 nm was determined for this stage. From the duration of a period, an average quenching time in the range of 10 ms was estimated. Further annealing (1100 K) causes some decrease in the amplitude of the current oscillation (Fig. 2E) and results in its total disappearance after the treatment at 1200 K. In this latter case, the average particle size grew up to 6.3 nm (Fig. 2F) and the $I$–$V$ curve exhibits a rather wide gap region ($\sim$2.2 eV) suggesting an insulating character of the detected area. It is worth remarking that nearly the same shape of spectra were detected on the terraces of the clean $TiO_2(1\,1\,0)-(1\times 2)$ surface, as it was presented in an earlier paper from our laboratory [4]. This observation is in harmony with the above conclusion that the Pt nanoparticles became entirely encapsulated when annealing above 1000 K [14,15].

Oscillations in the tunnelling current were also reported by Xi et al. on partially oxidized Si(1 0 0) and Si(1 1 1) surfaces [20]. The authors explained their observation by the capture and emission of individual electrons in/from the traps formed on $Si/SiO_x$ interface. In our case, the parallel appearance of the decoration state and the current oscillation suggest nearly the same explanation.

Fig. 3 shows characteristic $I$–$V$ curves detected above the central point of the post-grown Pt particles of different sizes (A: 6.1 nm; B: 9.5 nm; C: 28 nm; D: 17.5 nm). By comparing the zero-current regimes detected above the hexagonal particles (A–C), it can be deduced that an increase of the Pt crystallites results in an enhanced gap, although one would expect an opposite behaviour, i.e. a more metallic character for the larger crystallites. This contradiction may be explained by the formation of a $TiO_x$ decoration thin film on the top facet of the crystallites, as found earlier [14,15,19]. It is also interesting that the smaller rectangular shape crystallite exhibits a more restricted gap than the larger hexagonal one (Figs. 3C and D). To interpret this latter feature, we may assume that the interface between the rectangular particle and the substrate contains more oxygen-deficient sites than in the case of the hexagonal ones and/or the covering layer is less perfect [14,15,19].

## 4. Conclusions

The $I$–$V$ spectra recorded above the Pt nanoparticles grown in different sizes have shown that an increase in the average diameter of the Pt particles does not result in a more metallic character. This surprising behaviour may be explained by the formation of a $TiO_x$ decoration layer on top of the crystallites above 900 K. It was also observed that the STS spectra recorded above partially decorated Pt particles exhibit periodic current oscillations. This feature may be explained by the formation of electron trap states at the metal/oxide interface which emit and capture electrons to/from the tunnelling current.

## Acknowledgements

The authors gratefully acknowledge the support of the Hungarian Scientific Research Foundation through T29952, TS40877 and T32040 projects.

## References

[1] Bäumer M, Freund H-J. Prog Surf Sci 1999;61:127.
[2] Bifone A, Casalis L, Riva R. Phys Rev B 1995;16:11043.
[3] Radojkovic P, Schwartzkopff M, Enachescu M, Stefanov E, Hartmann E, Koch F. J Vac Sci Technol B 1996;14(2):1229.
[4] Berkó A, Solymosi F. Langmuir 1996;12:1257.
[5] Berkó A, Hakkel O, Szökő J, Solymosi F. Surf Sci 2002;000:000.
[6] Onishi H, Iwasawa Y. Surf Sci 1994;313:L783.
[7] Fischer S, Munz AW, Schierbaum KD, Göpel W. J Vac Sci Technol B 1996;14(2):961.
[8] Cocks ID, Guo Q, Williams EM. Surf Sci 1997;390:119.
[9] Benett RA, Poulston S, Stone P, Bowker M. Phys Rev B 1999;59:10341.

[10] Li M, Hebenstreit W, Diebold U. Phys Rev B 2000;61(7):4926.
[11] Pesty F, Steinrück HP, Madey TE. Surf Sci 1995;339:83.
[12] Steinrück HP, Pesty F, Zhang L, Madey TE. Phys Rev B 1995;51:2427.
[13] Berkó A, Ulrych I, Prince KC. J Phys Chem B 1998;102:3379.
[14] Dulub O, Hebenstreit W, Diebold U. Phys Rev Lett 2000;84(16):3646.
[15] Jennison DR, Dulub O, Hebenstreit W, Diebold U. Surf Sci 2001;492:L677.
[16] Berkó A, Klivényi G, Solymosi F. J Catal 1999;182:511.
[17] Berkó A, Soylmosi F. Surf Sci 1998;400:281.
[18] Berkó A, Szökő J, Solymosi F. Solid State Ion 2001;141–142:197.
[19] Berkó A, Szökő J, Solymosi F. Surf Sci 2003, in press.
[20] Xie F, Sun M, von Blanckenhagen P. Surf Sci 2000;454–456:1031.